

Bandlike and localized states at extended defects in silicon

W. Schröter, J. Kronewitz, U. Gnauert, F. Riedel, and M. Seibt

*Universität Göttingen, IV. Physikalisches Institut and Sonderforschungsbereich 345, Bunsenstrasse 13-15,
D-37073 Göttingen, Germany*

(Received 7 August 1995)

We show that electronic states at extended defects in semiconductors can be classified as bandlike or localized using deep-level transient spectroscopy (DLTS), when electron equilibration at the defect is taken into account. We compare computer simulations of DLTS with data for 60° dislocations and for NiSi_2 platelets in silicon and find narrow point defect clouds in the first and a two-dimensional metal or a metal ring in the second example.

Spatially extended, many-electron defects in semiconductors may be associated with deep-lying electronic states in the band gap, and thereby significantly affect charge-carrier density, mobility, and lifetime. Furthermore, their interaction with point defects, i.e., their action as sinks or sources for intrinsic point defects and segregation centers for impurities, has created significant detrimental effects in device technology, but has also been utilized, e.g., for gettering of impurities.

Electronic states at extended defects originating in their long-range strain and electric fields may give rise to shallow bands,^{1,2} and can be observed by photoluminescence, optical absorption, double-spin resonance, microwave conductivity, and electric dipole spin resonance.³ The subject of this work is deep-lying states at extended defects in silicon. These states originate from the atomic structure of the defect (bandlike states) and from their interaction with point defects (localized states). Consequently, the density $N(E)$ of deep electronic states at an extended defect is the sum of its bandlike and its localized states.

At present the deep levels associated with a variety of point defects are well understood, but despite many years of sustained effort the electrical properties of extended defects such as, for example, dislocations remain open.^{3,4} This has to be ascribed to the absence of appropriate techniques.

Magnetic-resonance techniques give insight into the electronic structure of point defects on the atomic scale, and have substantially contributed to our knowledge of their electrical properties. For dislocations in silicon, three electron-paramagnetic-resonance (EPR) centers, whose identification has been controversial for more than two decades,⁵ are now attributed to screw dislocations, specifically to vacancies and vacancy chains in the core of their 30° partials.^{3,6} We are not aware of other extended defect investigations in silicon by EPR.

Deep-level transient spectroscopy (DLTS) (Ref. 7) is a powerful and well-established tool to investigate deep point-defect levels. For extended defects, however, DLTS produces data which cannot be interpreted unambiguously. Kimerling and Patel⁸ found an asymmetrical-broadened DLTS line associated with dislocations in silicon, which survived annealing at high temperatures

and could result from localized or from bandlike states. Symmetrical line broadening has been observed after plastic deformation of silicon,⁹ and ascribed to the effect of deformation-induced disorder on the energy level and capture cross section of point defects.¹⁰ A further specific feature is a logarithmic capture law in a certain range of filling pulse length t_p , i.e., $\Delta C_m \sim \ln(t_p)$ (ΔC_m is the DLTS line amplitude). Such a law has been observed for dislocations in Si,¹¹ GaAs,¹² and CdTe,¹³ and recently also for dislocations in strain-relaxed GeSi/Si heterostructures.¹⁴

The consistent interpretation of both odd line shape and logarithmic capture law is a longstanding open problem of semiconductor defect physics. Its solution is basic to distinguish between bandlike and localized states and also for an access to $N(E)$ of extended defects.

In this paper, we show that the origin and distribution of deep levels associated with extended defects can be understood in terms of the rate R_i at which the levels reach internal equilibrium compared with the rates R_c and R_e at which they attain equilibrium with the valence and conduction bands (see Fig. 1). The key point is to use R_i to define the two limiting cases of bandlike ($R_i \gg R_c, R_e$)

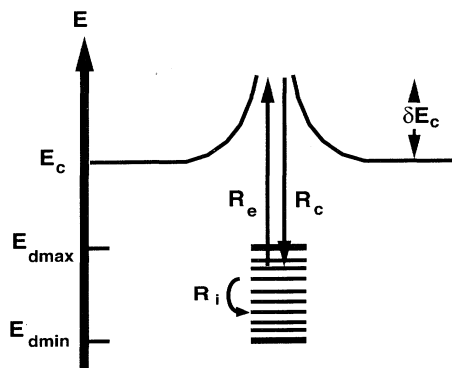


FIG. 1. Extended defect with deep states in the band gap exchanging electrons with the conduction band by electron emission (rate R_e) and electron capture (rate R_c). Introducing the internal equilibration rate R_i , the defect states are classified as bandlike ($R_i \gg R_e, R_c$) and localized ($R_i \ll R_e, R_c$).

and localized ($R_i \ll R_c, R_e$) states at extended defects, and to specify the differences of their DLTS characteristics by computer simulations. From the DLTS line shape we obtain a qualitative picture of $N(E)$.

Applying this analytic method to experimental data, we find that DLTS signals attributed to 60° dislocations in silicon¹⁵ originate from narrow point-defect clouds surrounding these dislocations due to elastic interaction. Finally, we report DLTS data associated with NiSi_2 platelets in n -type Si. We find that they are associated with one- or two-dimensional deep bands. To our knowledge this is the first time that an extended defect with deep bandlike states has been identified in silicon.

Consider n -type silicon with a dopant concentration N_0 , containing deep point defects ($N_d \ll N_0$). The capacitance transient $\Delta C(t)$ of a Schottky contact after increasing the bias voltage from a reduced value, at which the traps have been filled, is related to the local transient of occupied traps $\Delta n_d(z, t)$ by

$$\Delta C(t) = -\frac{C_0}{N_0} \frac{1}{w_0^2} \int_0^\infty \Delta n_d(z, t) z dz$$

(w_0 and C_0 are equilibrium values of the space-charge width and capacitance under reverse bias V_b , respectively; z is the distance from the metal-silicon interface).

The density of occupied traps $n_d(z, t) = N_d f(z, t)$ [$f(z, t)$ is the occupation probability] results from the capture of electrons with the rate R_c and from the emission of electrons with the rate R_e according to (see Fig. 1)

$$\frac{\partial f(z, t)}{\partial t} = R_c - R_e.$$

This equation has to be solved for the capture and emission periods separately.

For point defects, R_c and R_e are linear in f :

$$R_c = \sigma_n v_{th} n (1 - f),$$

$$R_e = e_n f$$

(v_{th} is the electron thermal velocity in the conduction band; the defect parameters are σ_n , electron-capture cross section, and e_n , electron emission rate). Then ΔC is exponentially dependent on time during capture and emission.

To simulate DLTS of extended defects we consider the effects of the capture barrier δE_c , of the density of states $N(E)$, and of internal equilibration on capture and emission rates. The logarithmic capture law has been shown to result from the Coulomb repulsion of free electrons by the defect,¹¹ described by a capture barrier δE_c :

$$R_c = \sigma_n v_{th} n (1 - f) \exp \left[\frac{-\delta E_c}{kT} \right].$$

In many cases an approximate expression is $\delta E_c = \alpha f$, with α being a constant.^{16,17}

It has been also shown that the shape of the DLTS line is almost independent of δE_c , when the extended defect states may be considered as degenerate.¹⁸ Consequently, line broadening indicates that the defect states are spread

over an energy range and are associated with an energy-dependent density of states $N(E)$.

For localized states at extended defects, variations of f result from transitions between each localized state and the conduction band:

$$\frac{\partial f(z, E, t)}{\partial t} = \sigma_n(E) v_{th} n [1 - f(z, E, t)] \times \exp \left[\frac{-\alpha F}{kT} \right] - e_n(E) f(z, E, t), \quad (1)$$

where F is the total occupation.¹⁹ For our simulations, we shall assume $\sigma_n(E)$ to be independent of E .

For bandlike states at extended defects, we approximate f at any time by a Fermi distribution with a quasi-Fermi-level E_{qF} . Then multiplication with $N(E)/N_d$, with $N_d = \int_0^\infty N(E) dE$, and integration over E yields a relation for $F(z, t)$:

$$\frac{\partial F(z, t)}{\partial t} = \sigma_n v_{th} n [1 - F(z, t)] \exp \left[\frac{-\alpha F}{kT} \right] - R_e(E_{qF}), \quad (2)$$

with

$$R_e(E_{qF}) = \int_0^\infty dE \frac{N(E)}{N_d} e_n(E) \times \left[1 + \exp \left[\frac{E + \alpha F - E_{qF}}{kT} \right] \right]^{-1}.$$

To compare with experimental data¹⁵ we have performed computer simulations for point-defect clouds in an inhomogeneous elastic strain field, and for one- and two-dimensional bandlike states. The figures show those results, which reproduce the relevant features of the measured DLTS lines.²⁰

Point defects, whose atomic radii are different from that of silicon, interact elastically with dislocations,²¹ and

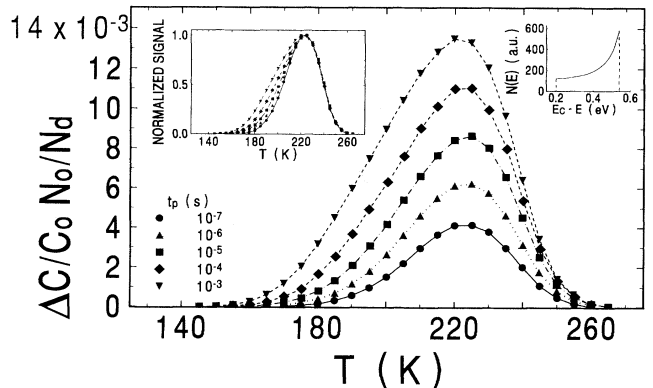


FIG. 2. Computer-simulated DLTS lines for a point defect cloud formed in the elastic stress field of 60° dislocations in n -type silicon [point defect: level $E_c - E_i^{(0)} = 0.70$ eV, misfit $\epsilon = 0.085$; $\sigma_n = 3 \times 10^{-14}$ cm², $D_{\text{eff}} = D = 6.5$ eV (Ref. 22), $E_{\text{dmin}} = E_c - 0.54$ eV, $E_{\text{dmax}} = E_c - 0.20$ eV, $\alpha = 0.4$ eV; $1/(t_e + t_p) = 17$ s⁻¹, $V_b - V_p = 0$ V, and $V_b = 4$ V]. The outer radius of the cloud has been taken as 1.1 nm (see text).

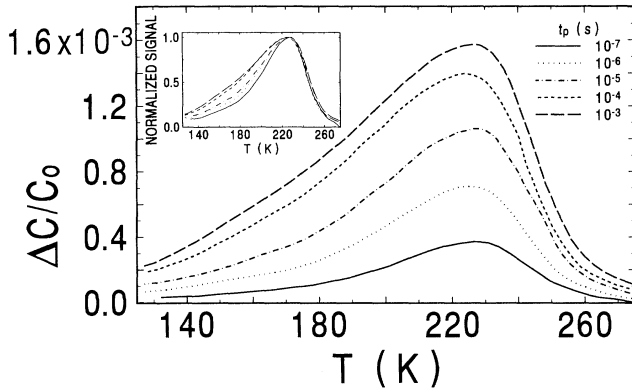


FIG. 3. Measured DLTS lines for 60° dislocations in *n*-type silicon [dislocation density: $5 \times 10^6 \text{ cm}^{-2}$; $N_0 = 4.5 \times 10^{14} \text{ P}^-$ atoms/ cm^3 , $1/(t_e + t_p) = 17 \text{ s}^{-1}$, $V_b - V_p = 0 \text{ V}$, and $V_b = 4 \text{ V}$] (Ref. 15).

may accumulate at the dislocation. Through the deformation potential D (Ref. 22) it also affects the width of the band gap. If D is different for the conduction-band edge and point-defect level, the emission rate varies in the strain field of the dislocation. Describing this relative variation by an effective deformation potential D_{eff} , we estimate a density of localized states $N(E_i)$ for the point-defect cloud as given in the inset of Fig. 2.

Results of our computer simulations for point-defect clouds are presented in Fig. 2. When compared with experimental data for 60° dislocations in *n*-type silicon, shown in Fig. 3, we note that there exists a large t_p range, for which (i) the position of the line maximum stays constant, and (ii) the maximum and high- T side of the line are related to t_p by $\Delta C \sim \ln(t_p)$. Radii of point-defect clouds which are generated by the strain field of dislocations fall into the range of at most a few nm.²¹ Our simulations show that the broadening of the DLTS line rapidly disappears when the cloud is expanded to beyond 1 nm.

Bandlike states of extended defects exhibit basic differences from features (i) and (ii). As an example, we show in Fig. 4 lines of a two-dimensional electron system [$N(E) = \text{const}$ for $E_{d\text{min}} \leq E \leq E_{d\text{max}}$] simulated using Eq. (2) and also our experimental results for NiSi₂ platelets in *n*-type Si. These platelets form during rapid quenching ($\dot{T} \geq 10^3 \text{ K/s}$) from high temperatures ($T \geq 850^\circ\text{C}$). The NiSi₂ platelets are coherent, and consist of two NiSi₂{111} layers; the interface to the silicon matrix consists of Si—Si bonds. They are metastable, since the Ni atoms have a sevenfold coordination instead of eightfold in bulk NiSi₂. Details of the structure have been described elsewhere.²³ We note that simulated and experimental data define a large t_p range for which the position of the line maximum shifts to lower temperatures with increasing t_p , and the high- T sides almost coincide. The

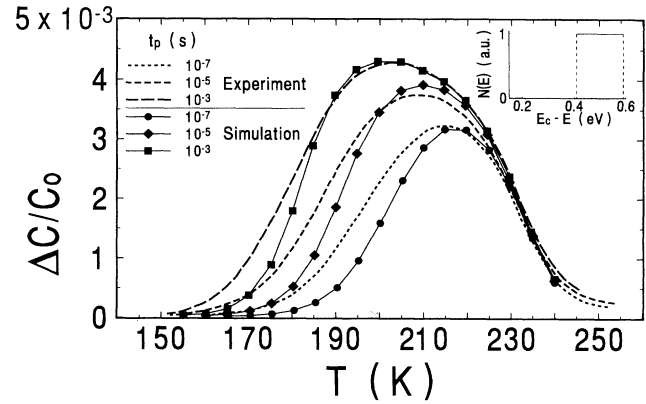


FIG. 4. Comparison of measured DLTS lines for NiSi₂ platelets [radius 20 nm] in *n*-type silicon ($N_0 = 1 \times 10^{15} \text{ P}^-$ atoms/ cm^3 , $1/(t_e + t_p) = 68 \text{ s}^{-1}$, $V_b - V_p = 0 \text{ V}$, and $V_b = 4 \text{ V}$) with computer simulated lines for a distribution $N(E) = \text{const}$ of extended states ($\sigma_n = 6 \times 10^{-13} \text{ cm}^2$, $E_{d\text{min}} = E_c - 0.59 \text{ eV}$, $E_{d\text{max}} = E_c - 0.41 \text{ eV}$, $\alpha = 0.3 \text{ eV}$, and $N_d/N_0 = 0.23$).

electrical activity of the platelet could originate in this specific interfacial structure.

However, associated with this interfacial structure is a dislocation bounding the precipitate, which has Burgers vector of type $a/4\langle 111 \rangle$. The unusual core of this dislocation could as well be electrically active. Whether the electronic structure of the platelet is appropriately described by a two-dimensional metal or by a metal ring remains open.

We mention that recently broad DLTS lines have been found to be associated with copper silicide platelets in silicon²⁴ and dislocations in strain-relaxed GeSi/Si heterostructures.¹⁴ Their variation with filling pulse length exhibits the same features which we have described for NiSi₂ platelets and attributed to bandlike states.

To summarize, by taking into account internal equilibration at extended defects we have demonstrated by computer simulation that DLTS allows to classify defect states as bandlike or localized. Using this approach we find that 60° dislocations in silicon are surrounded by point-defect clouds, with radii of the order of 1 nm. NiSi₂ platelets are associated with deep bandlike states from a two-dimensional metal or a metal ring.

Beyond these applications our approach allows us to study the interaction between point and extended defects. This opens a way of looking at technologically important processes such as gettering and relaxation of interfaces, and scientifically important processes such as pipe diffusion.

We gratefully acknowledge valuable discussions with K. Ahlborn and H. Hedemann.

- ¹V. Celli, A. Gold, and R. Thomson, *Phys. Rev. Lett.* **8**, 96 (1962).
- ²H. Teichler, *Lattice Defects in Semiconductors 1974*, IOP Conf. Proc. No. 23 (Institute of Physics, London, 1975), p. 374.
- ³H. Alexander and H. Teichler, in *Material Science and Technology*, edited by W. Schröter (VCH, Weinheim, 1991), Vol. 4, p. 249.
- ⁴See, e.g., R. Labusch and W. Schröter, *Lattice Defects in Semiconductors 1974* (Ref. 2), p. 56; *J. Phys. (Paris) Colloq.* **40**, C-6 (1979); **44**, C-4 (1983); A. Ourmazd, *Contemp. Phys.* **25**, 251 (1984); *Structure and Properties of Dislocations in Semiconductors 1989*, IOP Conf. Proc. No. 104 (Institute of Physics, London, 1989); *Phys. Status Solidi A* **138** (1993).
- ⁵See, e.g., *Izv. Akad. Nauk SSSR, Ser. Fiz.* **51** (1987) [*Bull. Acad. Sci. USSR. Phys. Ser.* **51** (4) (1987)].
- ⁶C. Kisielowski-Kemmerich, *Phys. Status Solidi B* **161**, 11 (1990).
- ⁷D. V. Lang, *J. Appl. Phys.* **45**, 3023 (1974).
- ⁸L. C. Kimerling and J. R. Patel, *Appl. Phys. Lett.* **34**, 73 (1979).
- ⁹P. Omling, E. R. Weber, L. Montelius, H. Alexander, and J. Michel, *Phys. Rev. B* **32**, 6571 (1985).
- ¹⁰C. Kisielowski and E. R. Weber, *Phys. Rev. B* **44**, 1600 (1991).
- ¹¹T. Figielski, *Solid State Electron.* **21**, 1403 (1978).
- ¹²T. Wosinski, in *Defect Control in Semiconductors*, edited by K. Sumino (North-Holland, Amsterdam, 1990), p. 1465.
- ¹³F. Gelsdorf and W. Schröter, *Philos. Mag. A* **49**, L35 (1984).
- ¹⁴P. N. Grillot, S. A. Ringel, E. A. Fitzgerald, G. P. Watson, and Y. H. Xie, *J. Appl. Phys.* **77**, 676 (1995); **77**, 3248 (1995).
- ¹⁵J. Kronewitz and W. Schröter, *Izv. Akad. Nauk SSSR, Ser. Fiz.* **51**, 682 (1987) [*Bull. Acad. Sci. USSR, Phys. Ser.* **51** (4), 51 (1987)].
- ¹⁶V. B. Shikin and N. I. Shinkina, *Phys. Status Solidi A* **108**, 669 (1988).
- ¹⁷R. Labusch and W. Schröter, in *Dislocations in Solids*, edited by F. R. N. Nabarro (North-Holland, Amsterdam, 1980), Vol. 5, p. 127.
- ¹⁸W. Schröter, I. Queisser, and J. Kronewitz, *Structure and Properties of Dislocations in Semiconductors 1989* (Ref. 4), p. 75.
- ¹⁹Note that the capture barrier depends on the *total occupation F* leading to a coupling of differential equations which has not been considered in previous works (cf. Ref. 9).
- ²⁰For one- and two-dimensional systems and point defect clouds we verified that the basic differences in DLTS-line characteristics for bandlike and localized states do not result from the particular shape of $N(E)$ chosen for the simulations presented in the figures.
- ²¹R. Bullough and R. C. Newman, in *Progress in Semiconductors*, edited by A. F. Gibbons and R. E. Burgers (Heywood, London, 1963), p. 99.
- ²²D. L. Dexter and F. Seitz, *Phys. Rev.* **86**, 964 (1952).
- ²³M. Seibt and W. Schröter, *Philos. Mag. A* **59**, 337 (1989).
- ²⁴M. Griess, Ph.D thesis, Göttingen, 1991.